文章编号：1001-9014(2023)02-0267-09

DOI:10.11972/j.issn.1001-9014.2023.02.018

Optimization of structural parameters of a 1.06 μm non-polarization mode-locked fiber laser

ZHANG Jia-Rui[1,2], WANG Ji[2,3], HE Xing-Kai[1], SHEN Qi-Hao[1], FAN Qi[1], ZHOU Ding-Fu[1], WANG You[1*]

(1. Southwest Institute of Technical Physics, Chengdu 610046, China;
2. School of Physics, Changchun University of Science and Technology, Changchun 130022, China;
3. Department of Mathematics and Theories, Peng Cheng Laboratory, Shenzhen 518000, China)

Abstract: A mode-locked fiber laser using Semiconductor Saturable Absorber Mirrors (SESAMs) is one of the popular candidate seed light sources for the construction of picosecond pulse fiber amplifier. In this paper, the influence of the fiber length of a gain fiber, the reflectance of the Fiber Bragg Grating (FBG), the modulation depth, the unsaturated loss, and the saturation flux of SESAMs, the mode field radii of single-mode transmission fibers and a single-mode gain fiber, on the output pulse characteristics, have been theoretically analyzed using the nonlinear Schrodinger equations. The characteristics of the pulse and the spectrum of an outputted laser have also been investigated theoretically. According to the simulation results, we built an ytterbium-doped mode-locking fiber laser system based on the non-polarization-maintaining linear cavity and a SESAM. Without any compensation for intra-cavity dispersion and external polarization control, a stable mode-locked pulse laser output has been achieved with the center wavelength of 1.06 μm, the pulse width of less than 12.51 ps, the spectral width of 0.32 nm, the repetition rate of 37 MHz, and the output power of 2 mW, respectively. The spectral edges of laser pulses appear smooth in our experiment, and the spectral distribution is close to the Gaussian shape. Finally, the overall structure of the near-infrared mode-locked fiber laser has been optimized by the systematic simulation. The mode-locked fiber laser introduced in this paper has a compact non-polarization-maintaining fiber structure, simple intra-cavity configuration with fewer components, high-quality output pulse correlation characteristics, which might provide a practical seed light source with the excellent performance for the next-generation picosecond pulse fiber lasers.

Key words: non polarization maintaining fiber, Gaussian linear spectrum, mode-locked fiber laser, structural optimization

1.06 μm结构参数最优化非保偏锁模光纤激光器

张家瑞[1,2], 王 蓟[2,3], 何幸锴[1], 沈琪皓[1], 范 琪[1], 周鼎富[1], 王 漱[1*]

(1. 西南技术物理研究所,四川 成都 610046;
2. 长春理工大学 物理学院,吉林 长春 130022;
3. 鹏城实验室 数学与理论部,广东 深圳 518000)

摘要:采用半导体可饱和吸收镜的锁模光纤激光器是构建皮秒脉冲光纤放大器的热门候选种子光源之一。本文利用非线性薛定谔方程从理论上分析了单模传输光纤和单模增益光纤的模场半径、增益光纤的光纤长度、光纤布拉格光栅的反射率、半导体可饱和吸收镜的调制深度、非饱和损耗和饱和通量对输出脉冲特性的影响。对输出激光的脉冲和光谱特性也进行了理论研究。根据仿真结果,搭建了基于非保偏线型腔和SESAM的掺镱锁模光纤激光器系统。在没有任何腔内色散补偿和外部偏振控制的情况下,获得了中心波长为1.06 μm、脉冲宽度小于12.51 ps、光谱宽度为0.32 nm、重复频率为37 MHz、输出功率为2 mW的稳定锁模脉

Received date: 2022-10-26, **revised date**: 2023-01-08　　**收稿日期**:2022-10-26,**修回日期**:2023-01-08

Foundation items: This work was supported by the National Key Research and Development Program of China (No. 2021YFA0718803), Sichuan Science and Technology Plan, China (No. 2022YFG0352).

Biography: Zhang Jia-Rui (1996-), Male, Liaoning Fuxin, assistant engineer of Southwest Institute of Technical Physics, master's degree, mainly engaged in the research of mode-locked fiber lasers and amplifiers.

[*] **Corresponding author**: E-mail: youwang_2007@aliyun.com

冲激光输出。在我们的实验中,激光脉冲的光谱边缘平滑,光谱分布非常接近高斯线型。最后,通过系统的仿真,近红外锁模光纤激光器的整体结构得到了优化。本文介绍的锁模光纤激光器具有紧凑的非保偏光纤结构、精简的腔内配置和较少的元器件、高质量的输出脉冲相关特性,有望为下一代皮秒脉冲光纤激光器提供性能优异的实用化种子光源。

关 键 词:非保偏光纤;高斯线型光谱;锁模光纤激光器;结构优化

中图分类号:TN2 **文献标识码**:A

Introduction

SESAMs, composed of a Saturable Absorber (SA) and a Bragg reflector, are the new mode-locked devices developed by the procedure of Metal-Organic Chemical Vapor Deposition (MOCVD). Compared with the mode-locking technology with a SA[1], a Nonlinear Polarization Rotation (NPR)[2], and a Nonlinear Amplifying Loop Mirror (NALM)[3], which are seriously affected by the environment and have more complex structures, the SESAM mode-locking technology has even higher stability and controllability and is easier to practically apply. Such regime plays an important role in the construction of picosecond fiber lasers.

Since 1992, Keller et al., first realized the passive mode-locking of solid-state lasers by using a Fabry-Perot etalon SA, SESAMs have undergone several innovations[4]. At present, SESAMs have been widely used in the realization of pulse fiber lasers[5, 6] and pulse solid-state lasers[7-8]. Since then, many researchers have paid their attentions in such lasers[9, 10]. In the mode-locked fiber laser based on a SESAM, ring cavity[11] and linear cavity[12] are commonly used. In 2008, Ori Katz et al. built an all-fiber picosecond pulsed fiber laser using a SESAM[13]. The dispersion in the cavity was compensated by a chirped fiber grating, and the polarization state in the cavity was controlled by a polarization controller. Finally, a 1.06 μm mode-locked pulse laser with the pulse width of 3.8 ps was obtained, and the spectrum shape of outputted pulses exhibited a non-Gaussian distribution. Such a laser was amplified as a seed source, which had the great influence on the spectral characteristics of the amplified pulse. In 2016, Wang Zi-Wei et al., developed a high peak-power picosecond photonic crystal fiber amplifier using a SESAM mode-locked fiber laser as the seed source[14]. After multi-stage amplifications, a high-powered pulse laser was obtained with the pulse width of 30 ps and the peak power of 2.94 MW. The output characteristics of the seed light are not well satisfactory, which brings about obvious distortion in amplified pulses. In 2018, Sun Jiang et al. built an all-polarization-maintaining ytterbium-doped fiber laser with a linear cavity based on the SESAM mode-locking[15]. The chirped fiber Bragg grating (CFBG) was used to compensate dispersion, and the all-polarization-maintaining structure was used to control the polarization state in the cavity, and the fiber focusing device was used to spatially couple the SESAM. Finally, the mode-locked pulse laser was obtained with the center wavelength and pulse width of 1.03 μm and 4.26 ps, respectively. The frequency domain output characteristics of the pulse are not satisfactory, and its spatial coupling SESAM mode is harmful to the integrity of such a fiber laser. Its all-polarization-maintaining fiber structure greatly increases the price of the system. In addition, there are many studies on fiber amplifiers using SESAM-based mode-locked fiber lasers as the seed source. However, most of the SESAM-based mode-locked fiber lasers are somewhat complicated and expensive. Additionally, the improvement of outputted characteristics of mode-locked pulses has not been mentioned in time domain and frequency domain. The frequency-domain output characteristics of a mode-locked fiber laser are the key factors to obtain the stable mode-locked pulse output. The higher the edge smoothness of the outputted spectrum is, and the closer the shape is to the ideal line, the more stable the output power of a mode-locked fiber laser is, and the more difficult the losing-lock becomes, the easier the amplified pulses with better output characteristics in the subsequent amplification are obtained. During constructing an ideal seed source for high-power pulsed fiber lasers, it is necessary to optimize the overall structure of a SESAM mode-locked fiber laser under the premise of ensuring the stable output, and to maintain the satisfied output characteristics in both time domain and frequency domain.

In order to make the correlation characteristics of outputted pulses for a mode-locked fiber laser with the compact linear cavity more ideal, and to further reduce the development cost, we build a SESAM-based passively mode-locked fiber laser with the non-polarization maintaining linear cavity by the use of the theoretical simulation in this paper. The cavity length can be further shortened by using the ytterbium-doped gain fiber with the relatively high absorption coefficient, where any polarization controllers have not been employed. Without compensating the dispersion in the cavity, we obtained the stable mode-locked pulse output with the center wavelength of 1.06 μm, the pulse width of less than 12 ps, the 3 dB spectral width of 0.32 nm, the repetition rate of 37 MHz, and the output power of 2 mW, respectively. The spectral edge of the pulse is smooth, and the spectral shape is very close to the Gaussian distribution. The similar research reports have been proved to be very rare. This paper might put forward to a valuable route for the commercialization of the next-generation SESAM mode-locked fiber lasers.

1 Theoretical analyses

The structure of a linear-cavity fiber laser using the SESAM-based mode-locking is shown in Fig. 1. An Yb-doped gain fiber with high absorption coefficient was

used as the lasing element. A SESAM is used as both the mode-locking device and the high reflector. A FBG is used as the wavelength selection device. The resonant cavity is composed of the SESAM and FBG. A 975 nm semiconductor laser is used as the pump source. The output pump light is directly coupled to the resonant cavity by a Wavelength Division Multiplexer (WDM). The mode-locked laser pulses are outputted from the FBG end, which was acted an output coupler.

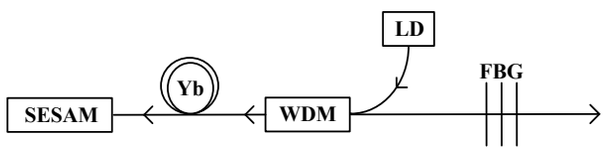

Fig. 1 The schematic illustration of a SESAM mode-locked fiber laser with the linear cavity
图1 线型腔SESAM锁模光纤激光器示意图

When the pulse is transmitted in a single-mode fiber, the relationship is followed by the nonlinear Schrodinger equation as expressed by

$$\frac{\partial \mathrm{A}}{\partial z}+i\frac{1}{2}\beta_2\frac{\partial^2 \mathrm{A}}{\partial \mathrm{T}^2}-\frac{\beta_3}{6}\frac{\partial^3 \mathrm{A}}{\partial \mathrm{T}^3}=i\gamma|\mathrm{A}|^2\mathrm{A}-\frac{1}{2}\alpha\mathrm{A}\ , \quad (1)$$

where A is the pulse intensity, T is time, β_2 is the second-order group velocity dispersion, β_3 is the third-order group velocity dispersion, γ is the nonlinear coefficient, α is the absorption coefficient, respectively. When the pulse is transmitted in the Yb-doped fiber, the variation of refractive index n_2 is specified by the electric polarization rate of doped ions χd :

$$\Delta n = n_2|\mathrm{E}|^2+\frac{i\tilde{\alpha}}{2k_0}+\frac{\chi_d}{2n} \quad , \quad (2)$$

where E is energy. After considering the bandwidth limitation caused by the gain, the group velocity dispersion, β_2^{eff}, of the gain fiber can be expressed by

$$\beta_2^{eff}=\beta_2+ig\mathrm{T}_2^2 \quad , \quad (3)$$

where T_2 is the dipole relaxation time, g is the gain coefficient following

$$g=\frac{g_0}{1+\mathrm{E}_p/\mathrm{E}_{sat}} \quad , \quad (4)$$

where E_p is the instantaneous pulse energy and E_{sat} is the gain saturation energy, respectively.

Therefore, when the pulse is transmitted in the fiber doped with rare earth ions, the physical relationship can be given by the following Ginzburg-Landau equation:

$$\frac{\partial \mathrm{A}}{\partial z}+i\frac{1}{2}\left(\beta_2+ig\mathrm{T}_2^2\right)\frac{\partial^2 \mathrm{A}}{\partial \mathrm{T}^2}-\frac{\beta_3}{6}\frac{\partial^3 \mathrm{A}}{\partial \mathrm{T}^3}= i\gamma|\mathrm{A}|^2\mathrm{A}+\frac{1}{2}\left(g-\alpha\right)\mathrm{A} \quad . \quad (5)$$

Two terms on the right side of the equation characterize the nonlinear effect and gain-loss relationship, respectively.

2 Simulation results

2.1 Influence of the radius of mode field

The radius of mode field is a parameter to describe the energy transmission concentration of a single-mode fiber, which is important in estimating the fiber loss and dispersion. Figure 2 is diagramed the output intensity of mode-locked pulses with different mode field radii of a single-mode fiber with 2.2, 2.95, 3.1, 3.25, and 3.75 μm, respectively. Figure 3 illustrates the change trend of the pulse width and spectral width for different mode field radii. As the mode field radius of the single-mode fiber increases from 2.2 to 3.75 μm, the Full Width at Half Maximum (FWHM) of the output mode-locked pulse broadens from 9.39 to 12.88 ps, and the FWHM in spectral merely decreases from 5.69 to 4.83 nm, respectively. Figures 2 and 3 show that one can obtain the relatively narrow pulse width using a single mode fiber with the small mode field radius. The single-mode

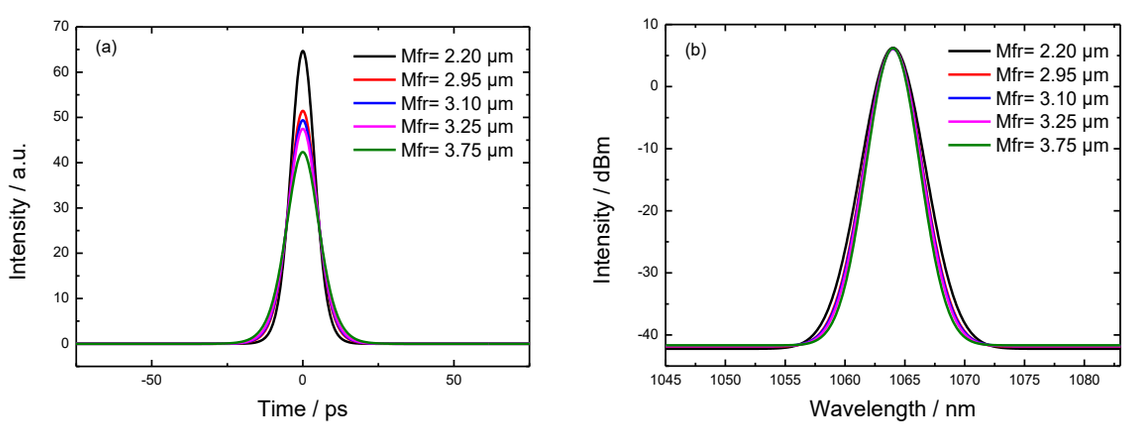

(a) (b)

Fig. 2 Influence of the mode field radius of a single-mode fiber on characteristics in both the time domain (a) and the frequency domain (b) for different linear cavity mode-locked laser pulses
图2 单模光纤的模场半径对不同线型腔锁模激光脉冲的时域(a)和频域(b)特性的影响

fiber with a larger mode field radius has a larger core diameter, which will reduce the laser power density and weaken the nonlinear effect in the cavity, resulting in the gradual narrowing of the spectrum. According to the principle of time bandwidth product, the increase of the pulse width and the decrease of the pulse amplitude can be observed in time domain. By considering the pulse density drops for a big cross section, it is judicious in selecting a single mode fiber with the small core in which the nonlinear effect is not serious.

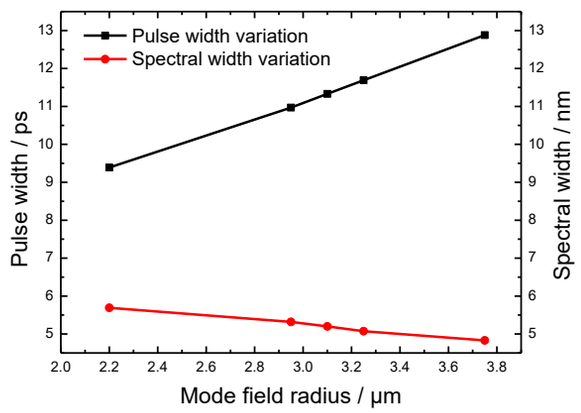

Fig. 3 Influence of the mode field radius of a single-mode fiber on the pulse width and spectral width
图3 单模光纤的模场半径对脉冲宽度和光谱宽度的影响

2.2 Influence of the length of a gain fiber

In Fig. 4, the influence of the length of a gain fiber on the output pulse characteristics is shown. The absorption coefficient of the gain fiber is 1200 dB/m. The dispersion coefficient of the gain fiber is -35.905 ps/nm*km. When the selected length of a gain fiber is increased from 0.11 to 0.17 m, the spectral width increases gradually from 2.84 to 8.36 nm because the nonlinear effect gradually enhances. Since the pump energy can be absorbed more sufficiently for a gain fiber as long as 0.17 m, the pulse width reduces to 7.87 ps. Figure 5 shows the variation trend of the pulse width and spectral width with seven kinds of gain fiber lengths. If the length of a gain fiber is too short, the pulse width becomes too big and the mode-locking even cannot maintain. If the length of a gain fiber is too long, the nonlinear effect becomes more serious and is harmful to the amplification process. Therefore, we select the length region of the gain fiber as 0.12-0.14 m, which is proper to achieve the suitable pulse width and spectral width at the same time.

2.3 Influence of the reflectance of a FBG

The reflectance of a FBG influences the energy returned to the resonant cavity and outputted pulse characteristics. The output features of mode-locked pulses are shown in Fig. 6 with the FBG reflectance of 20%, 50%, 70%, 80%, and 90%. When the reflectance of a FBG is increased from 20 to 90%, the spectral width gradually decreases from 10.02 to 5.77 nm. The gradual narrowing of the spectral width will further reduce the pulse broadening caused by dispersion. One can see from Fig. 6 that the even narrower spectral width and pulse width can be obtained by appropriately increasing the reflectance of a FBG. The variation trend of the pulse width and spectral width are also investigated for 14 kinds of reflectance as shown in Fig. 7. The simulation results show that when the reflectance is 80%, the pulse and spectral widths are 9.65 ps and 7.24 nm, respectively. When the reflectance is raised to 90%, the pulse and spectral widths are 9.39 ps and 5.77 nm, respectively. Thus, we select the reflectance region of the FBG as 80%-90%, which is appropriate to simultaneously achieve the short pulse width and suitable spectral width.

2.4 Effect of the modulation depth of a SESAM

The greater the modulation depth of a SESAM is, the stronger the ability of a SESAM to absorb the weak

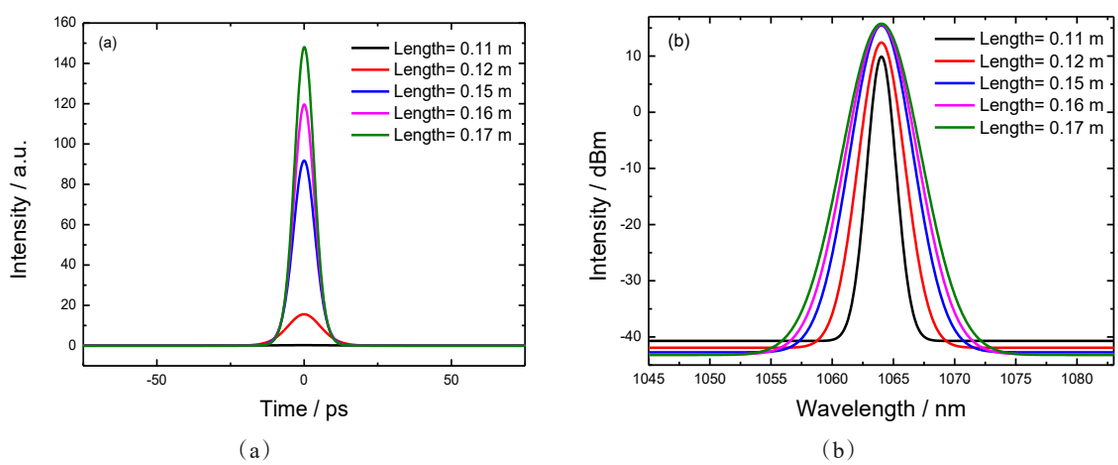

(a) (b)

Fig. 4 Influence of the gain fiber length on characteristics in both the time domain (a) and the frequency domain (b) of different linear cavity mode-locked laser pulses
图4 增益光纤的长度对不同线型腔锁模激光脉冲的时域(a)和频域(b)特性的影响

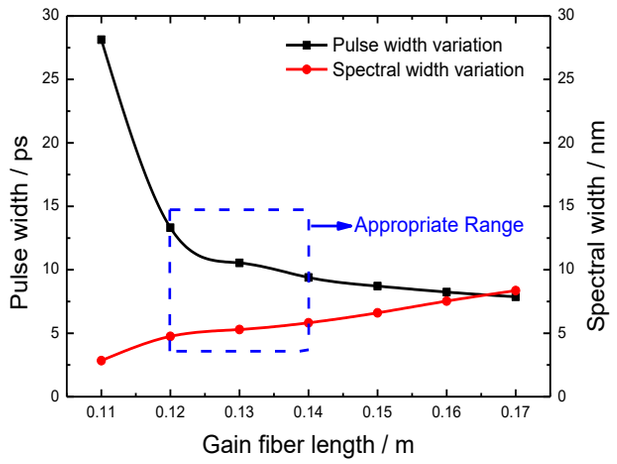

Fig. 5 Effect of the gain fiber length on the pulse width and spectral width
图5 增益光纤的长度对脉冲宽度和光谱宽度的影响

signal becomes, and the easier the realization of mode-locked self-starting is. Figure 8 shows the output of mode-locked pulses when the modulation depth of a SESAM is assumed to be 1%, 10%, 20%, 35%, and 45% according to the actual parameters from the SESAM maker. In Fig. 9, the trend of the pulse width and spectral width with the different SESAM modulation depths. As the modulation depth of a SESAM is increased from 1 to 45%, the pulse width is decreased from 17.59 to 8.09 ps, and the spectral width is broadened from 5.88 to 6.5 nm. From the plot, one can observe that within a certain range, the larger the modulation depth of a SESAM, the narrower the pulse width becomes. Actually, a large modulation depth will bring the great unsaturated loss, and the small modulation depth will increase the difficulty of mode-locked self-starting. In this study, considering the balance of the pulse width and spectral width, we think the suitable region of the modulation depth of a SESAM is of 15% - 25%.

2.5 Effect of the unsaturated loss of a SESAM

Unsaturated loss is one kind of depletions which exists even in the saturated state of a SESAM. Insufficient reflectivity, rough surface, impurities, etc., of a SESAM can all lead to unsaturated loss. In Fig. 10, the output characteristics in both the time domain and frequency domain are given with the unsaturated loss of a SESAM of 0.7%, 10%, 15%, 20%, and 25%. It is obvious that the pulse width varies a little and the spectral width is almost unchanged for different unsaturated losses.

In Fig. 11, the variation trend of the pulse width and spectral width is plotted as the function of unsaturated loss of a SESAM. As the unsaturated loss of a SESAM is increased from 0.7% to 25%, the pulse width decreases from 9.85 ps to 8.49 ps, and the spectral width is narrowed from 6.53 nm to 6.07 nm. Although the pulse width and spectral width decrease slightly with the increase of unsaturated loss of an SESAM, the outputted power will decrease rapidly because of the big unsaturated loss. Therefore, it is better for a user to select a SESAM with low unsaturated loss.

2.6 Effect of the saturation flux of a SESAM

The saturation flux is the photon energy per absorption cross section when the reflectance of a SESAM is 1/e of its modulation depth, which is directly related to the pump power required to achieve mode-locking self-starting. In Fig. 12, the output intensity of mode-locked pulses is shown when the saturation flux of a SESAM is 15, 25, 50, 100, and 130 μJ/cm^2.

Fig. 13 shows the relationship between the pulse width and spectral width and the SESAM saturation flux. As the saturation flux of a SESAM increases from 15 to 130 μJ/cm^2, the pulse width of the mode-locked pulse is obviously broadened from 8.73 to 14.6 ps, and the spectral width is narrowed from 6.95 to 5.03 nm. The broadening in the pulse width and the narrowing in the spectrum correspond to the continuous enhancement of nonlinear effects of a SESAM. It can be seen that the saturation flux has the more obvious effect on the pulse width

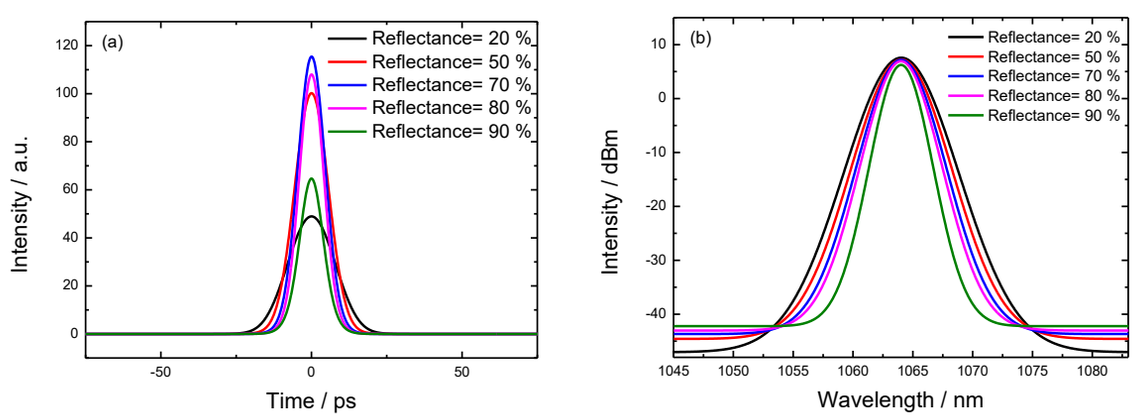

(a) (b)

Fig. 6 Influence of the FBG output reflectance on characteristics in both the time domain (a) and the frequency domain (b) of different linear cavity mode-locked laser pulses
图6 光纤布拉格光栅的反射率对不同线型腔锁模激光脉冲的时域(a)和频域(b)特性的影响

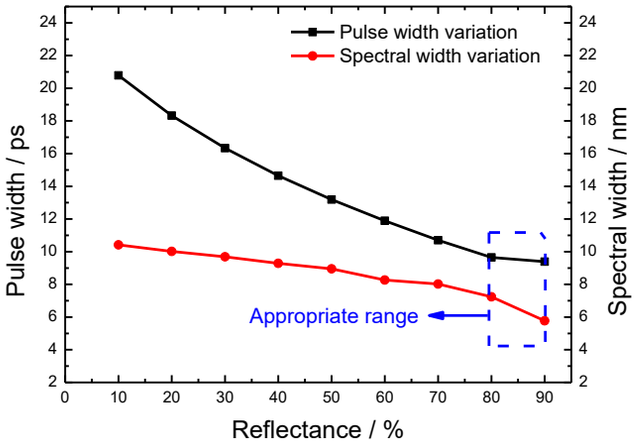

Fig. 7 Influence of the reflectance of a FBG on the pulse width and spectral width
图7 光纤布拉格光栅的反射率对脉冲宽度和光谱宽度的影响

than on the spectral features. If the saturation flux is too small, the mode-locking self-starting will become somewhat difficult. If the saturation flux is too large, the nonlinear effect will be serious. Therefore, it is appropriate to select a SESAM with the saturation flux less than 50 μJ/cm^2 as a mode-locked device. Generally, a SESAM with the relatively small saturation flux is popular to obtain a mode-locked laser pulse with the even narrower pulse width.

3 Experiments and analyses

3.1 Experimental system

Using theoretical simulation results analyzed by an approach of control variation, we finally determined all suitable parameters of an Yb-doped fiber laser. Next, we undertook the experimental verification using a system as shown in Fig. 14. A FBG (Ruike Huatai Electronic Tech. Corp. Ltd.) with the reflectance of 80%, reflection bandwidth of 0.31 nm, and center wavelength of 1.06 μm, was selected as the cavity output coupler. A

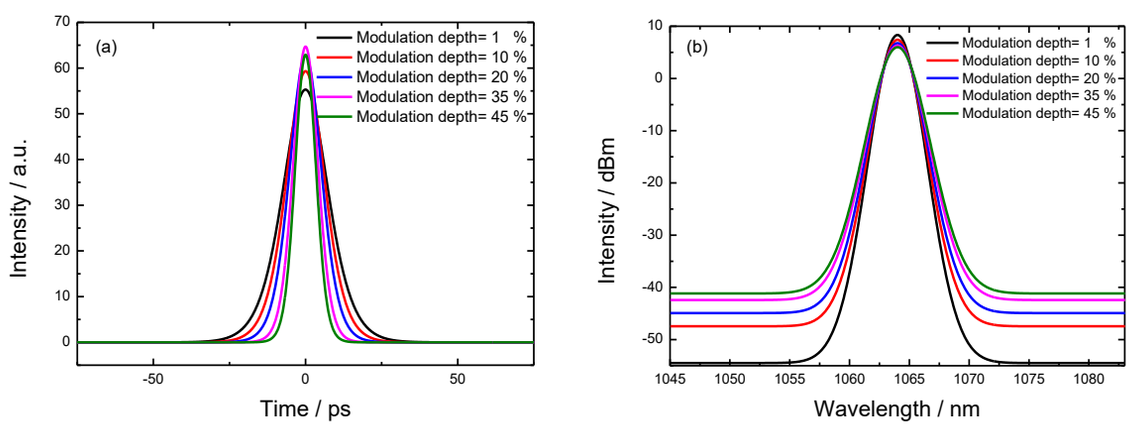

(a) (b)

Fig. 8 Influence of the SESAM modulation depth on characteristics in both the time domain (a) and the frequency domain (b) of different linear cavity mode-locked laser pulses
图8 SESAM的调制深度对不同线型腔锁模激光脉冲的时域(a)和频域(b)特性的影响

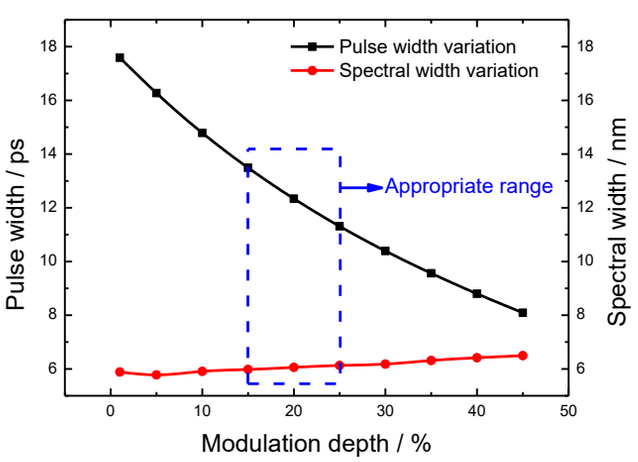

Fig. 9 Effect of the modulation depth of a SESAM on the pulse width and spectral width
图9 SESAM的调制深度对脉冲宽度和光谱宽度的影响

gain fiber (Yb1200-4-125, n-LIGHT Inc.) with the length of 0.13 m and a SESAM (SAM-1064-28-15ps-x, German BATOP Ltd.) were utilized as the laser medium and mode-locked device, respectively. The modulation depth, saturation flux, and reflection bandwidth are 18%, 30 μJ/cm^2, and 70 nm, respectively. Such a SESAM is especially suitable for constructing a multi-band mode-locked laser. The transmission fiber (HI1060, Corning Inc.) is employed as tail fibers and a transmission jumper. Note that the length of a tail fiber was strictly controlled as short as possible.

3.2 Experimental results and analyses

When the power of the 976 nm pump LD was gradually increased from 0 to 24 mW, the unstable pulse lasing can be observed through an 8 GHz oscilloscope. When the pump power is increased to 27 mW, a pulse cluster is generated. When the pump power is increased

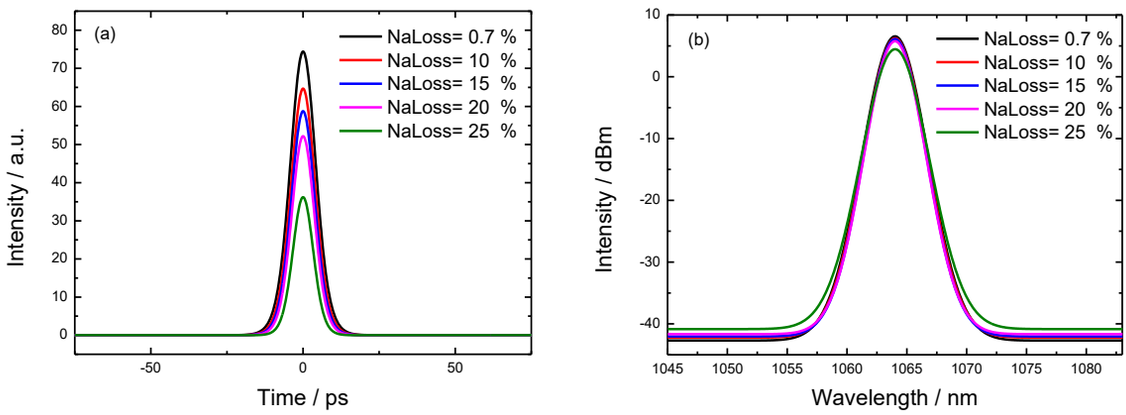

(a) (b)

Fig. 10 Influence of the SESAM unsaturated loss on characteristics in both the time domain (a) and the frequency domain (b) of different linear cavity mode-locked laser pulses
图 10 SESAM 的非饱和损耗对不同线型腔锁模激光脉冲的时域(a)和频域(b)特性的影响

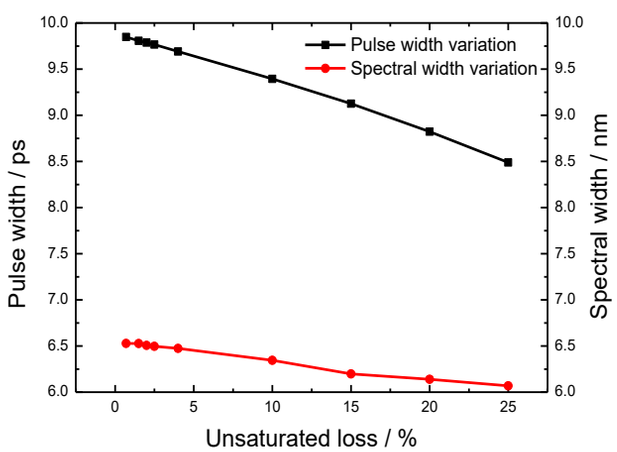

Fig. 11 Effect of unsaturated loss of SESAM on the pulse width and spectral width
图 11 SESAM 的非饱和损耗对脉冲宽度和光谱宽度的影响

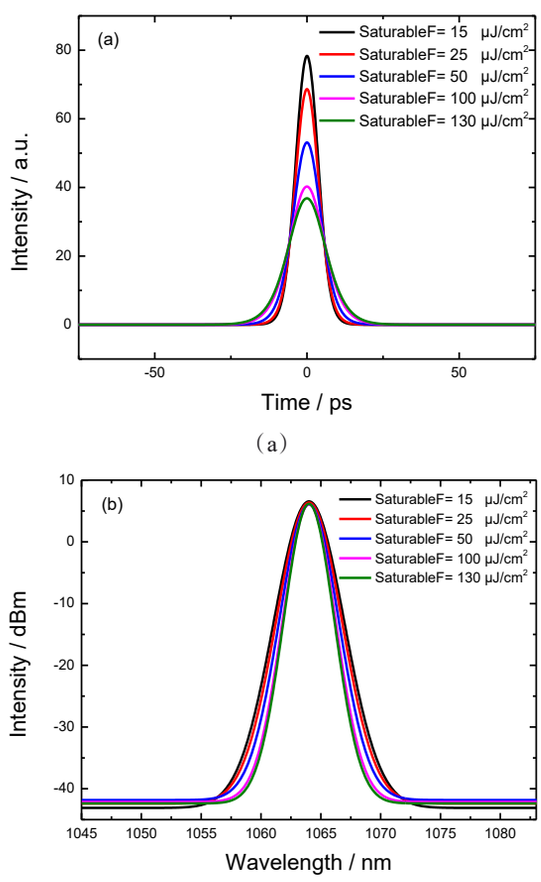

(a) (b)

Fig. 12 Influence of SESAM saturation flux on characteristics in both the time domain (a) and the frequency domain (b) of different linear cavity mode-locked laser pulses
图 12 SESAM 的饱和通量对不同线型腔锁模激光脉冲的时域(a)和频域(b)特性的影响

to 40 mW, a stable mode-locked pulse output can be achieved with the repetition rate of 37 MHz. The output average power was measured as 0.45 mW by a power meter (Newport1830-R). The spectral width of the mode-locked pulse was measured as 0.22 nm@3 dB at the center wavelength of 1.06 μm by using a spectrometer (AQ6373-10-H, YOKOGAWA Inc.). The spectral width is much narrower than the theoretical results because the reflection bandwidth of the selected FBG is as narrow as 0.31 nm. The measured pulse sequence and spectrum are shown in Figs. 15 (a) and (b) for stable mode locking, respectively. It can be seen that the spectral edge of the mode-locked pulse is quite smooth, and the overall shape is very close to the Gaussian distribution. The input-output power characteristics are plotted for our mode-locked fiber laser in Fig. 16.

Next, the pump power was gradually increased to 65 mW, and the output power is increased to 2 mW. After working for 5 hours, we observed that the mode-locked pulse maintained stably, and the output power has no obvious fluctuation. When the pump power was increased to 66 mW, the regular single pulse output changed to an irregular double pulse one for our mode-

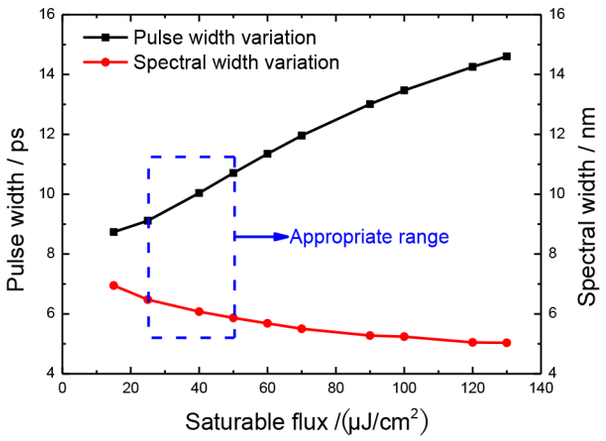

Fig. 13 Effects of saturation flux of SESAM on the pulse width and spectral width
图13 SESAM的饱和通量对脉冲宽度和光谱宽度的影响

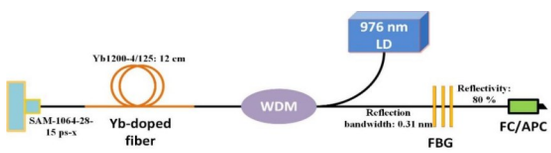

Fig. 14 Structural diagram of the experimental setup
图14 实验装置的结构图

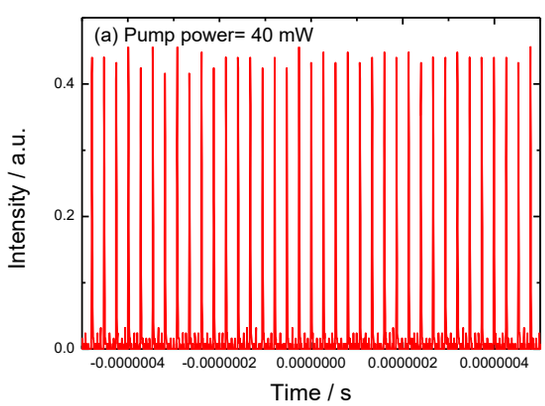

(a)

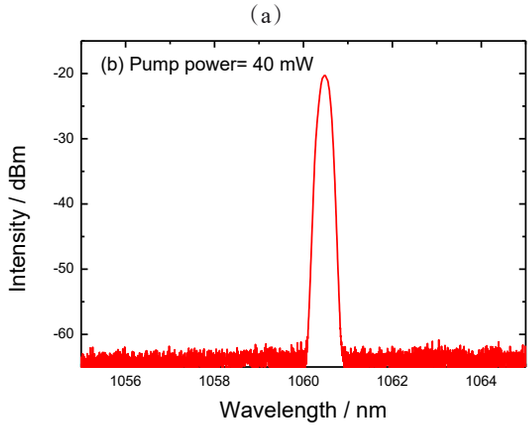

(b)

Fig. 15 Pulse train (a) and spectrum (b) of a mode-locked laser with the pump power of 40 mW
图15 泵浦功率为40 mW的锁模激光器的脉冲序列(a)和光谱(b)

locked laser, and the time interval between two mode-locked pulses is about 0.027 μs, as shown in Fig. 17. The reason of presence of double pulses is thought to derive from the high-order harmonic mode-locking. Note that the spectral characteristics of the output pulse had no obvious variation at that time.

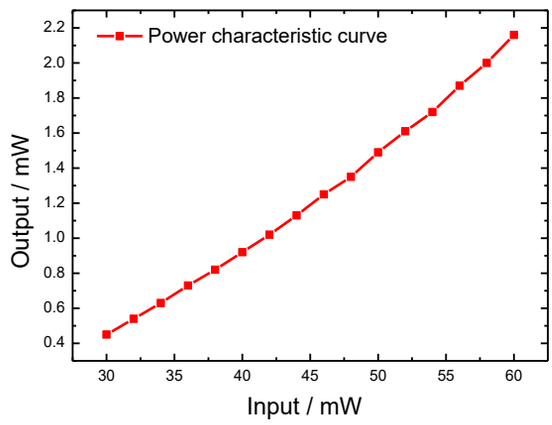

Fig. 16 Output power as a function of the input power
图16 输入-输出功率特性曲线

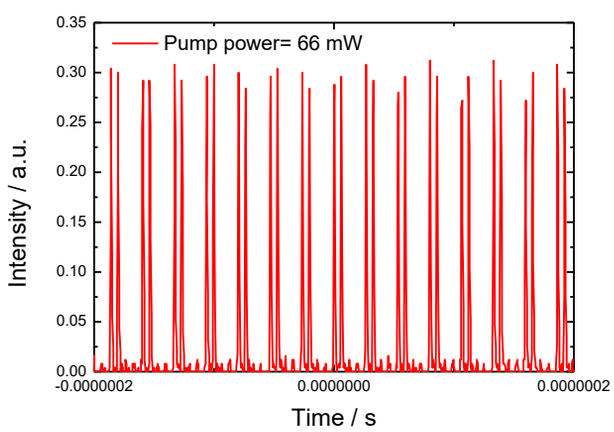

Fig. 17 Generation of mode-locked pulses with the pump power of 66 mW
图17 泵浦功率为66 mW时,产生多脉冲锁模

The spectra of the mode-locked pulses are also compared for different pump power as shown in Fig. 18. It is found that the 3 dB spectral width is slightly broadened from 0.22 to 0.32 nm with the increase of the pump power due to the nonlinear effect in the cavity. However, all the spectral curves remain the good Gaussian-shape.

Because the output power of the seed source is low and the peak power is not high enough, the pulse width cannot be detected by the autocorrelation instrument. In our study, the pre-amplifier module was added to enlarge the outputted power on purpose, and the pulse width can be therefore measured. The pump power of the seed and pre-amplifier modules are 60 and 100 mW, respectively. The output pulse width was measured as 12.51 ps by use of an autocorrelator (A·P·E Ltd.) as shown in Fig. 19. The pulse train after the pre-amplification was still stable, and the overall shape of the spectrum was confirmed to be

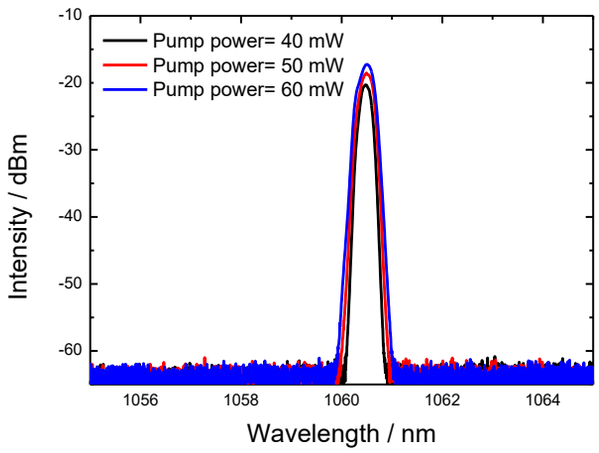

Fig. 18 Spectra of mode-locked pulses with the pump power of 40, 50, and 60 mW
图 18 泵浦功率为 40、50 和 60 mW 的锁模脉冲光谱

less influenced by nonlinear effects such as amplified spontaneous emission (ASE) and self-phase modulation (SPM). Considering the positive dispersion and nonlinear effects introduced by the pre-amplifier stage, the pulse width of the seed light should be less than 12.51 ps.

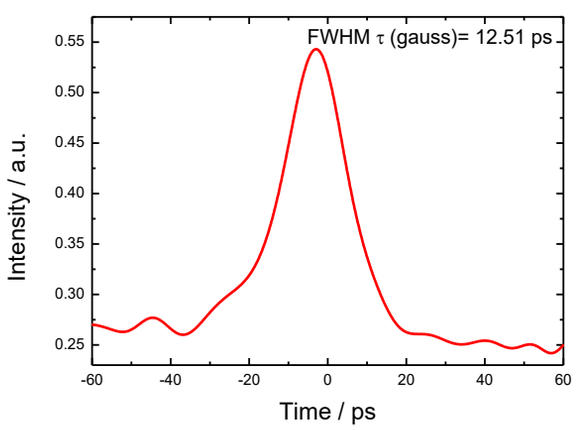

Fig. 19 Mode-locked pulse measured by the autocorrelation procedure
图 19 通过自相关仪测量的锁模脉冲

4 Conclusions

The mode field radius of a single-mode fiber, the length of a gain fiber, the reflectivity of a FBG, and the main parameters of a SESAM in the linear cavity are theoretically analyzed by the numerical simulation for a mode-locked fiber laser. A subtraction optimization of the laser structure has been realized based on the theoretical results, and a mode-locked fiber laser with the non-polarization maintaining linear cavity has been built for experimental verification. Finally, we obtained a satisfactory mode-locked laser source with the center wavelength of 1.06 μm, the pulse width of less than 12.51 ps, the 3 dB spectral width of 0.32 nm, the repetition rate of 37 MHz, and the output power of 2 mW, respectively. It is believed that such a mode-locked fiber laser might be valuable as a seed source for the construction of an industrial picosecond pulse laser system in the near future.

References

[1] Sathiyan S, Velmurugan V, Senthilnathan K, *et al*. All-normal dispersion passively mode-locked Yb-doped fiber laser using MOS_2-PVA saturable absorber[J]. *Laser Physics*, 2016, **26**(5).
[2] Chi Jun-Jie, Li Ping-Xue, Yang Chun, *et al*. Theoretical and experimental study on all-normal-dispersion Yb-doped mode-locked fiber lasers[J]. *Chinese Physics B*, 2013, **22**(4):44204-044204.
[3] Jiang Tong-Xiao, Cui Yi-Fan, Lu Pei, *et al*. All PM fiber laser mode locked with a compact phase biased amplifier loop mirror[J]. *IEEE Photonics Technology Letters*, 2016, **28**(16):1786-1789.
[4] Keller U, Miller DA, Boyd GD, *et al*. Solid-state low-loss intracavity saturable absorber for Nd:YLF lasers: an A-FPSA[J]. *Optics Letters*, 1992, **17**(7):505-507.
[5] Lai Xue, Li Jian-Feng, Luo Hong-Yu, *et al*. High power passively Q-switched Er^{3+}-doped ZBLAN fiber laser at 2.8 μm based on a semiconductor saturable absorber mirror[J]. *Laser Physics Letters*, **2018 15**(8).
[6] Wang Zhao-Kun, Zou Feng, Wang Zi-Wei, *et al*. Tunable and switchable narrow bandwidth semiconductor-saturable absorber mirror mode-locked Yb-doped fiber laser delivering different pulse widths[J]. *Chinese Physics Letters*, 2016, **33**(3):034202.
[7] Gaponenko, Maxim, Metz, et al. SESAM mode-locked red praseodymium laser[J]. *Optics Letters*, 2014, **39**(24):6939-6941.
[8] Gong M, Yu Hai-Juan, Wushouer X, *et al*. Passively mode-locked Nd: YVO4 picosecond laser with oblique incidence on SESAM[J]. *Laser Physics Letters*, 2010, **5**(7).
[9] Kim J W, Park S, Kim G H, *et al*. A 1030 nm all-PM SESAM mode-locked dissipative soliton fiber oscillator and its amplification with Yb-doped fiber and a Yb: YAG thin rod[J]. *Laser Physics*, 2022, **32**(10).
[10] Bai Yang-Bo, Xiang Wang-Hua, Zu Peng, *et al*. Tunable dual-wavelength passively mode-locked Yb-doped fiber laser using SESAM[J]. *Chinese Optics Letters*, 2012, **10**(11).
[11] Wang Yong-Gang, Ma Xiao-Yu, Fu Sheng-Gui, *et al*. Passive Q-switched mode locking of double-clading Yb fiber laser with ion-implanted GaAs[J]. *Acta Physica Sinica*, 2004, **53**(6): 1810-1814.
[12] Li Ping-Xue, Yao Yi-Fei, Chi Jun-Jie, *et al*. 980-nm all-fiber mode-locked Yb-doped phosphate fiber oscillator based on semiconductor saturable absorber mirror and its amplifier[J]. *Chinese Physics B*, 2016(8):84207-084207.
[13] Ori Katz, Yoav Sintov. Strictly all-fiber picosecond ytterbium fiber laser utilizing chirped-fiber-bragg-gratings for dispersion control [J]. *Optics Communications*, 2008, **281**(10), 2874 - 2878.
[14] Wang Zi-Wei, Wang Zhao-Kun, Zhou Feng, *et al*. High-peak-powerrod-type photonic crystal fiber amplifier for picosecond pulses [J]. Chinses Journal Of Lasers, 2016, **43**(10):17-23.(王子薇,王兆坤,邹峰,等.高峰值功率皮秒脉冲棒状光子晶体光纤放大器[J].**中国激光**),2016,**43**(10):17-23.
[15] Sun-Jiang, Hou Lei, Lin Qi-Meng, *et al*. All-polarization maintaining mode-loched Yb-doped fiber laser with chirped fiber bragg grating[J]. Acta Photonica Sinica, 2018, **47**(01):119-124.(孙江,侯磊,林启蒙,等.基于啁啾光纤布拉格光栅的掺镱保偏锁模光纤激光研究[J].**光子学报**),2018,**47**(01):119-124.